Desalination and Water Treatment
www.deswater.com
doi: 10.1080/19443994.2013.815586

52 (2014) 6519–6529
October

Taylor & Francis
Taylor & Francis Group

A QICAR model for quantifying connection between metal ionic character and biosorption capacity of *Pleurotus eryngii*

Nan He, Wan Li, Heng Xu*

Key Laboratory of Bio-resources and Eco-environment (Ministry of Education), College of Life Science, Sichuan University, Chengdu, Sichuan 610064, China
Tel. +86 28 85414644; Fax: +86 28 85418262; email: xuheng64@sina.com

Received 16 February 2013; Accepted 9 June 2013

ABSTRACT

Quantitative ion character–activity relationship (QICAR) was used for quantifying connection between metal ionic characteristics with maximum biosorption capacity (q_{max}). q_{max} of *Pleurotus eryngii* was determined by Langmuir isotherm decreasing in the order of: $Pb^{2+} > Cr^{3+} > Cu^{2+} > Zn^{2+} > Cd^{2+} > Ni^{2+} > K^{+}$. In batch studies, Minimum Run Res V Design was used to determine the most significant medium factors. It was found that pH, biomass loading, and contact time manifest stronger influence on biosorption of Pb^{2+} and Cd^{2+}. In the 22 physiochemical characteristics of metal ions, Covalent Index $X_m^2 r$ was correlated best with q_{max} for all metal ions tested ($R^2 = 0.69$). Classifying metal ions appropriately could improve models and more ionic properties could be significantly correlated with q_{max}. It turned out that the best fitting parameter for divalent metal ions was $X_m^2 r$ ($R^2 = 0.93$) and for transition metal ions was $|\log K_{OH}|$ ($R^2 = 0.90$). Moreover, two-variable model had greater ability to improve the fitting result ($R^2 = 0.99$).

Keywords: Biosorption; Metal ionic character; QICAR; Mushroom fruit body

1. Introduction

Nowadays, heavy metal pollution of wastewater is becoming a worldwide environmental problem. Heavy metal has toxicity toward aquatic life, including plants, animals, microbes, and even be harm for the environment. Meanwhile, it has a great impact on human health. Many reports indicate that excessive intake of copper by humans may lead to severe mucosal irritation, hepatic and renal damage, capillary damage, gastrointestinal irritation, and central nervous system irritation [1]. Excessive zinc enters the human body and accumulates in the liver and kidneys resulting in hemochromatosis and gastrointestinal catarrh diseases. High concentration of nickel enters the body would cause cancers of the lungs, nose, and bone [2]. Thus, this heavy metal pollution crisis is extremely urgent. To solve the expanding problem, various methods have been employed to eliminate metal cations from aqueous solution, such as reverse osmosis, ion exchange, carbon adsorption, electroflotation, and chemical precipitation [3]. Adsorption method was widely researched and applied because of its high efficiency, limited pollution, and low cost. There are many factors that can influence adsorption capacity especially: metal ionic characteristics (e.g. atomic weight, ion radius, valence, etc.), the features of the adsorbents

*Corresponding author.

and adsorption conditions (e.g. pH, temperature, contact time, etc.) [4]. However, a large proportion of researchers have studied on reaction condition and adsorption mechanism of certain adsorbent rather than the influence of metal ionic character to the adsorption [5–7].

Quantitative structure activity–relationships (QSAR) is a method to establish the correlation between the bioactivity (e.g. toxicity or bioavailability), and chemical parameters of organic compounds in pharmacology and toxicology [8,9]. During the last few decades, some scientific researchers have studied correlations between physical and chemical properties of metal ions and their toxicity [10–13]. To predict metal toxicity, quantitative ion character–activity relationship (QICAR) have been developed by Newman and co-workers based on metal-ligand-binding tendencies [10,14,15]. QICAR can even be used for correlating metal ionic character with maximum biosorption capacity (q_{max}), since carboxyl, hydroxyl, amino, and hydrosulfuryl play momentous roles in biosorption and the mechanism of adsorbing heavy metal ion include complexation and ion exchange [16–19].

Biosorption is a novel technique which developed rapidly in recent years with its advantage of efficiently dealing with metal cations contaminated water. From plants to microorganism, different kinds of organisms have been used as adsorbent, such as lichen and bamboo [20,21]. Fungi are a sort of novel bioadsorbent which possess extraordinary ability to remove metal cations from aqueous solution due to its abundant materials source and excellent degradability [22,23]. As reported earlier, plenty kinds varieties, of fungi have been widely used as adsorbents to metal cations removal recently, such as Pb^{2+} and Cd^{2+} removed by *Amanita rubescens*, Cu^{2+} and Pb^{2+} uptakedused by *Lentinus edodes* [24,25]. In this study, we choose *Pleurotus eryngii* a kind of common mushrooms as the adsorbent to remove various toxic metals (Pb^{2+}, Cd^{2+}, Cr^{3+}, Cu^{2+}, Zn^{2+}, Ni^{+}, K^{+}). Factorial design was also used to screening many factors to find the important effect and interations [23]. QICAR models is created to deduce maximum biosorption capacity and to understand the metal–biomass interactions.

2. Materials and methods

2.1. Preparation of the biosorbent

Fresh *P. eryngii* was collected from a mushroom production site in the suburbs of Chengdu, China. It was washed with generous amounts of deionized water and dried in an oven at 50°C for 3d. Then, dried biosorbent was grounded with a pulverizing mill (Joyoung, JYL-350B, China) and sieved with a 200-mesh to a size <0.075 mm.

2.2. Metal solution

Stock metal solutions of 1,000 mg/L were prepared by dissolving appropriate amounts of $Pb(NO_3)_2$, $Cr(NO_3)_3{\cdot}9H_2O$, KNO_3, $Cu(NO_3)_2{\cdot}3H_2O$, $Zn(NO_3)_2{\cdot}4H_2O$, $Ni(NO_3)_2{\cdot}6H_2O$, and $Cd(NO_3)_2{\cdot}4H_2O$ (All reagents used here were analytical purity purchased from Changzheng Chemical Reagent company, Chengdu, China) in ultrapure water. The required working solutions of metal cations for the adsorption experiments were obtained by diluting each stock solution. Real concentration of metal ions in solutions was confirmed by flame atomic absorption spectroscopy (AAS, VARIAN, SpectrAA-220Fs, USA).

2.3. Biosorption experiments

According to pre-experiment, a series of flasks (150 ml) containing 50 ml metal solution were prepared for all the adsorption study. The pH was adjusted by adding HNO_3 (0.1, 1 M) and NaOH (0.1, 1 M) solutions. The adsorption studies were carried out in a shaker incubator (SUKUN, SKY-211B, China), and flame atomic adsorption spectrometry was used to measure the metal concentration of filtrated solution.

The removal rate and amount of adsorbed metal ions (Q_e) per gram of *P. eryngii* were calculated as follows:

$$\text{Removal rate } (\%) = 100 \times (C_i - C_e) \times 1/C_i \quad (1)$$

$$\text{Adsorption amount (mg/g): } Q_e = (C_i - C_e)V \times 1/M \quad (2)$$

where C_i and C_e are the metal ions concentrations (mg/L) initially and at a given time t, respectively; V is the volume of the heavy metal solutions (L); M is the weight of adsorbent (g). Experiments were conducted in triplicate and the average values were taken as a result.

2.4. Factorial design methodology

The factorial design method determines which factors have significant effects on a response as well as how the effect of one factor varies according to the level of the other factors [26,27]. In order to evaluate the factors that affected the removal rate (%) of metal ions, a Minimum Run Res V Design was applied. The 6 statistically significant main factors of the process

(temperature, pH, initial metal ions concentration, biomass loading, contact time, and agitation speed) were selected in our study. In the full factorial design, 32 experiments are required. However, fractional factorial design was chosen to analyze the effects of each variable on the adsorption of metallic ions could shortcut batch experiments to 22. Each factor was represented at two levels—high and low, denoted by (+1) and (−1) signs, respectively [28]. The factors and their respective level are summarized in Table 1.

2.5. Ion characteristics and model development

For the modeling experiment, 22 metal ionic physiochemical properties were chosen to be variables. These ionic characteristics were as follows: r (Å), AN, ΔE_0(V), ΔIP(eV), X_m, $|\log K_{OH}|$, $X_m^2 r$, Z^2/r, AN/ΔIP, σp, OX, AR, AW, IP, AR/AW, Z^*,Z^{*2}/r, N, Z/r^2, Z/AR^2, Z/r, Z/AR given in Table 2 [10,29,30].

The software Eviews 6.0 was used to perform regression models of q_{max} values with 22 metal ionic characteristics. The level of significance was set as $\alpha = 0.05$ and the following statistic parameters were computed: R = correlation coefficient, R^2 = coefficient of determination, R^2_{adj} = adjusted R^2, SE = standard error of regression, F ratio = F test, P = probability of significance; MAPE = mean absolute percent error between observed and predicted values in prediction.

2.6. Fourier transform-Infrared spectroscopic analysis

High-resolution ($0.1\,cm^{-1}$) Fourier transform-infrared (FT-IR) spectra for the biomass of *P. eryngii* (before and after the Pb^{2+} sorption) were recorded under vacuum on a VERTEX 80 v (Bruker optics). FT-IR spectrometer equipped with a DTGS (with KBr window) detector. Freeze-dried biomass was mixed with KBr powder, ground at room temperature and then compressed into a thin pellet.

Table 1
Experimental ranges and levels of the factors studied in the factorial design

Signal	Factor	Units	Levels and range	
			−1	+1
A	Temperature	℃	20	40
B	Initial metal ions concentration	mg/L	10	100
C	pH		2	5
D	Biomass loading	g/L	1	6
E	Agitation speed	rpm	50	200
F	Contact time	min	10	240

3. Results and discussion

3.1. Screening of significant effects

Factorial design was employed to reduce the total number of experiments in order to achieve the best overall optimization of the process. Pb^{2+} and Cd^{2+} were selected as sample to represent soft ions and borderline ions. The removal of Cd^{2+} and Pb^{2+} are presented in Table 3. The analysis of variance (ANOVA) for biosorption study of Pb^{2+} and Cd^{2+} ions with *P. eryngii* was used in order to ensure a good model. The normal curves for the adsorption of the ions showed the main significant factors in the adsorption of each metallic ion. Values of "Prob > F" less than 0.05 indicate model terms are significant (Table 4). The R^2 of 0.9034, 0.8518, and the adjusted R^2 of 0.8986, 0.8452 were in reasonable agreement for Pb^{2+}, Cd^{2+} removal. The models proposed are as follows:

$$\text{Pb(II) removal } (\%) = +0.361 + 0.029A + 0.032B - 0.166C + 0.130D + 0.079E + 0.143F \quad (3)$$

$$\text{Cd(II) removal } (\%) = +0.295 - 0.013A + 0.009B - 0.026C + 0.083D + 0.0150E + 0.063F \quad (4)$$

where A, B, C, D, E, and F were defined in Table 1. Based on Eqs. (3) and (4) pH, biomass loading and contact time have a main effect on the adsorption. The significant factors affecting the Pb^{2+}, Cd^{2+} adsorption can be observed in Fig. 1. It was found that for Pb^{2+}, temperature, pH, contact time, biomass loading, and agitation speed had a positive effect while initial ion concentration was negative. It can be observed that the decreasing of initial concentration and temperature lead to better results of adsorption of Cd^{2+}. Considering the conclusion mentioned above, temperature for 30℃, pH for 5, biomass loading for 6 g/L, agitation speed for 200 rpm were optimum combination for metal cations removal.

3.2. Maximum sorption capacity

The maximum sorption capacity (q_{max}) of metal ions was calculated by the Langmuir isotherm model which assumes that uptake takes place on a homogenous surface by monolayer sorption without any interaction between the adsorbed molecules. The linear form is expressed by the following equation.

Table 2
Values of metal ionic characteristics used in correlations

Properties	Nomenclature	Pb	Cd	Cr	Cu	Zn	Ni	K
AN	Atomic number	82	48	24	29	30	28	19
r (Å)	Pauling ionic radius (Å)	1.18	0.95	0.62	0.73	0.75	0.69	1.38
ΔIP(eV)	Change in ionization potential (eV)	7.61	7.91	14.46	12.57	8.57	10.52	4.34
ΔE_0(V)	Electrochemical potential of the ionand its first stable reduced state (V)	0.13	0.4	0.41	0.16	0.7618	0.23	2.92
Xm	Electronegativity	2.33	1.69	1.66	1.9	1.81	1.91	0.82
$\lvert\log K_{OH}\rvert$	Absolute value of log of the first hydrolysis constant	7.7	10.1	4	8	9	9.9	14.5
$X_m^2 r$	Covalent index	6.41	2.71	1.71	2.64	2.04	2.52	0.93
Z^2/r	The cation polarization force	3.39	4.21	14.52	5.48	5.33	5.8	0.72
AN/ΔIP	Atomic number/change in ionization potential	10.78	6.07	1.66	2.31	3.5	2.66	4.38
σ_p	Softness index	0.131	0.081	0.107	0.104	0.115	0.126	0.232
OX	Oxidation number	2	2	3	2	2	2	1
AR	Atomic radius	1.54	1.48	1.25	1.53	1.31	1.25	2.31
AW	Atomic weight	207.19	112.4	51.996	63.54	65.37	58.71	39.102
IP	Ionization potential	15.0322	16.908	30.96	20.2924	17.9644	18.16884	4.34066
AR/AW	The ratio between atomic radius and atomic weight	0.0074	0.0132	0.024	0.024	0.02	0.0213	0.0591
Z^*	Effective ion charge	19.8	16.4	11.35	14.25	14.9	13.6	7.4
Z^{*2}/r	The cation polarization force	297	274.449	198.118	282.03	267.482	237.128	41.173
N	The number of valence shell electrons	20	18	11	17	18	16	8
Z/r^2	The cation polarization force	1.417	2.216	7.732	3.753	3.55	4.201	0.525
Z/AR^2	The similar polarization force	0.843	0.913	1.92	1.183	1.165	1.28	0.187
Z/r	The cation polarization force	1.695	2.105	4.839	2.74	2.665	2.899	0.725
Z/AR	The similar polarization force	1.299	1.351	2.4	1.307	1.526	1.6	0.433

$$1/q_e = 1/q_{max} + 1/(q_{max}b)C_e \quad (5)$$

It could be transformed for fitting of the experimental data as following equation:

$$C_e/q_e = (1/q_{max})C_e + 1/(q_{max}b) \quad (6)$$

where q_e (mg/g) is the equilibrium metal uptake, C_e (mg/L) represents the concentration of solution at equilibrium, q_{max} (mmol/g) is the maximum adsorption and b (L/mg) is the Langmuir constant positive related to the energy of adsorption. The values of q_{max} for different metal ions were listed in Table 5.

It showed that q_{max} decreased in the following order: $Pb^{2+} > Cr^{3+} > Cu^{2+} > Zn^{2+} > Cd^{2+} > Ni^{2+} > K^+$ and presented *P. eryngii* might have prominent capacity to remove Pb^{2+} from liquid which was proved by some similar biosorbent [31]. Comparing with other biosorbent, *P. eryngii* displayed superiority to remove Pb^{2+} from solution. In this study, q_{max} of Pb adsorbed by *P. eryngii* was 0.412 mmoml/g, namely 85.284 mg/g. It's more than 75.8 mg/g of lichen (*Parmelina tiliaceae*) biomass [20] and 77.8 mg/g of bacterium *Pseudomonas* sp [32]. Several other studies also indicated this capacity order, for example, the bisorption affinity of *Tricholoma lobayense* was $Pb^{2+} > Cu^{2+} > Cd^{2+}$ [23] and biomass for biosorption of metal ions by *Rhizopus nigricans* was $Pb^{2+} > Cu^{2+} > Zn^{2+} > Ni^{2+}$ [33]. A study of biosorption of Cd(II) and Cr(III) from aqueous solution by moss (*Hylocomium splendens*) biomass also presented the maximum biosorption capacity (q_{max}) was $Cr^{3+} > Cd^{2+}$ [34]. According to the principal of HSAB (hard-soft-acid-base), soft ions(Pb^{2+}) mainly interact with the biological ligands via covalent bond, hard ions (K^+) mainly via electrostatic interaction [35,36] and borderline ions (Cd^{2+}, Cr^{3+}, Cu^{2+}, Zn^{2+}, Ni^{2+}) are variant. Cadmium cation was mainly removed through apparently chelation and nickel was mainly ion exchange [37,38]. It might explain the order of abovementioned uptake capacity.

Table 3
Factorial design experimental data

Std.	Factors						Responses (% removal)	
	A	B	C	D	E	F	Pb	Cd
1	20	10	2	6	50	10	79.2	48.7
2	20	10	2	1	200	10	26.1	24.5
3	20	100	2	1	200	10	92.8	68.5
4	40	10	2	6	50	240	41.9	28.1
5	20	100	2	6	200	10	36.7	25
6	40	100	5	1	50	240	39.6	23.4
7	40	100	2	1	50	10	48.4	15.2
8	20	100	2	6	50	240	67.5	24.3
9	20	100	5	1	50	10	24.4	21
10	20	100	5	6	200	240	74.8	68.1
11	20	10	5	6	50	240	77.3	23
12	40	10	5	1	50	10	92.7	80.9
13	40	10	2	6	200	240	10.2	17.3
14	20	10	5	6	200	10	24.5	38.4
15	20	10	2	1	50	240	40.7	43.9
16	40	100	5	6	50	10	34	12.8
17	40	100	2	6	200	240	15.3	26.2
18	40	100	5	1	50	10	9.1	14.7
19	40	10	2	1	200	240	89.6	69.6
20	40	10	5	6	200	240	26.3	11.8
21	40	100	5	1	200	10	80.1	48.9
22	20	10	5	1	200	240	12.1	19.5

Table 4
ANOVA for the regression model

Term	Sum of squares (SS)		*F*-Value		*P*-value	
	Pb	Cd	Pb	Cd	Pb	Cd
Model	1.36	0.62	23.32	12.13	<0.0001	<0.0001
A	0.012	0.007775	39.11	0.56	0.1487	0.2851
B	0.028	0.001259	2.84	0.08	0.0809	0.5210
C	0.51	0.47	2.5	48.71	<0.0001	<0.0001
D	0.43	0.064	38.27	9.60	<0.0001	0.0007
E	0.12	0.008	21.36	1.42	0.0013	0.2619
F	0.39	0.15	14.09	12.97	<0.0001	0.0027
Residual	0.13	0.09				
Cor. total	1.49	0.71				
R^2	0.9034	0.8518				
R^2_{adj}	0.8986	0.8452				

3.3. Correlation ionic properties with q_{max}

3.3.1. Models for all metal ions

The models were built with the q_{max} values of seven metal ions and their corresponding ionic properties by using software Eviews 6.0. The results revealed that among 22 kinds of parameter only 2 ($X^2_m r$, AW,) were statistical significant (at the level of significance 0.005) (Table 6). $X^2_m r$ showed the highest statistical significance, but only could explain 64% of the variation in q_{max} values. The relationship between q_{max} and $X^2_m r$ was depicted in Fig. 2(a).

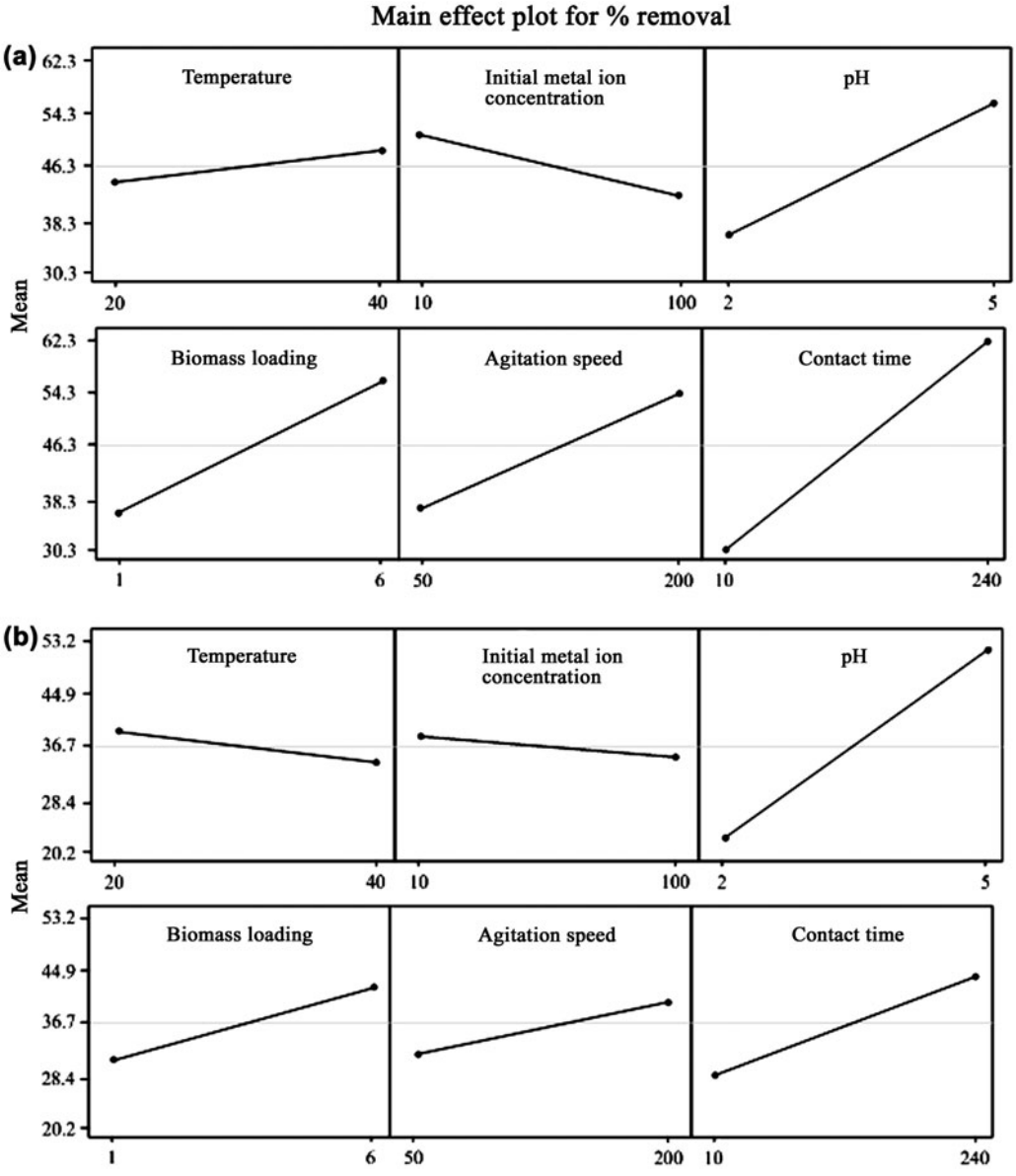

Fig. 1. Main effects plot for (a) the removal of Pb(II) and (b) removal of Cd(II) by *P. eryngii*.

Table 5
Maximum uptake capacity (q_{max}) by *P. eryngii*

Metal	q_{max} (mmoml/g)	R^2	Outer electronic configuration	Class
Pb^{2+}	0.412	0.932	$6s^2\ 6p^2$	Nontransition metal
Cr^{3+}	0.253	0.974	$3d^5 4s^1$	Transition metal
Cu^{2+}	0.217	0.933	$3d^{10} 4s^1$	Transition metal
Zn^{2+}	0.202	0.958	$3d^{10}\ 4s^2$	Transition metal
Cd^2	0.196	0.912	$4d^{10}\ 5s^2$	Transition metal
Ni^{2+}	0.183	0.967	$3d^8 4s^2$	Transition metal
K^+	0.112	0.982	$4s^1$	Nontransition metal

Table 6
Regression models of relationship between q_{max} and metal ion characteristics for all metal ions tested ($n = 7$)

Model (q_{max} =)	R^2	R^2_{adj}	SE	F	p	MAPE
1. $0.045X^2_m r + 0.076$	0.694	0.639	0.042	24.904	0.004	13.656
2. $0.001AW + 0.088$	0.564	0.492	0.457	15.059	0.012	21.042

Fig. 2(a) indicated the biosorption capacity of the biomass rise along with the Covalent Index Value of metal ion. Similar result was obtained by Brady for *Rhizopus arrhizus* and Chen for *Saccharomyces cerevisiae* [39,40], who both built the linear relation between q_{max} and and found out they were positively correlated. Nieboer and McBryde [41] introduced that Covalent Index had a tendency to form metal ionic complexes in aqueous solution. According to Nieboer, the greater the Covalent Index values the softer the metal ions. These ions were combined with the functional groups of biological in the order of S→N→O and easily formed stable complexes with the group including S and N like S^{2-}, RS^-, R_2S, CN^-, H^-, R^-, then less stabled R_2NH, R_3N,=N–, –CO–N–R, RNH_2 .On the contrary, hard ions firstly formed stable complexes with the group including O, such as ROH, $RCOO^-$, CO, ROR, HPO_4^{2-}, OH^-, O^{2-}, H_2O, NO^{3-} ,$ROSO_3^-$, CO_3^{2-}. Therefore, we can conclude that the covalent interactions between ions and organisms should not be neglected for its important effect in ion adsorption mechanism.

AW also had close bond with q_{max}. Some studies proved that with increasing atomic weight, the biosorption increased in the same order [42,43]. Javier Bayo indicated atomic weight can explain the affinity order for the four heavy metals was Pb(II) > Cu(II) > Ni(II) [42].

3.3.2. Models for divalent metal

When models were set up with only divalent metal ions, more ionic characteristics became statistical significant (AN, X_m, r(Å), Z^2/r, AN/ΔIP, N, Z/r^2, Z/r),

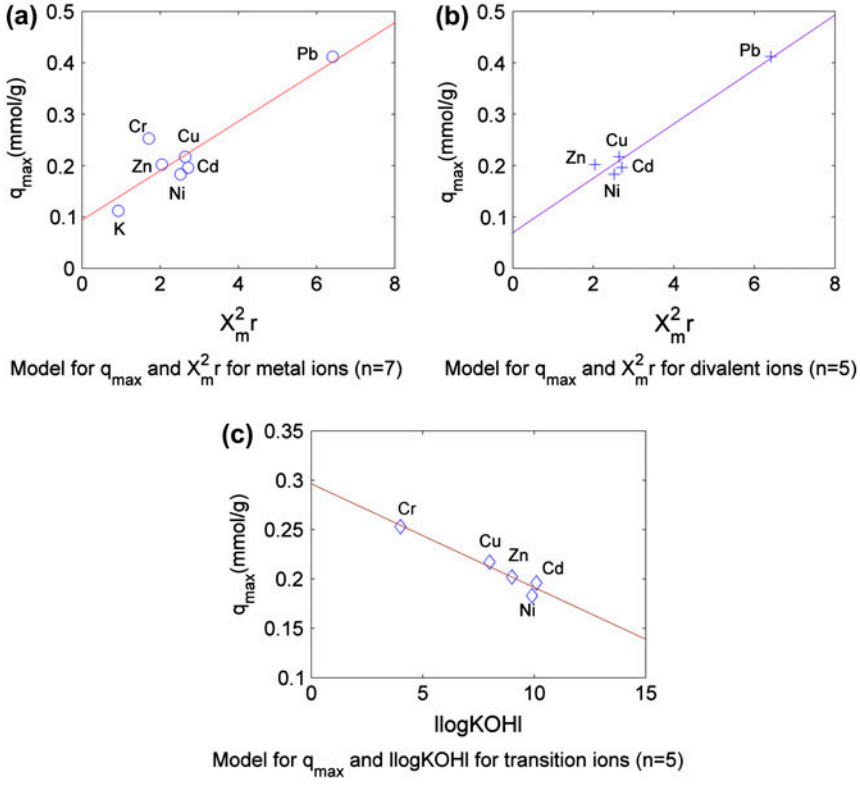

Fig. 2. Models for q_{max} and $X^2_m r$ for all metal ions ($n = 7$) (a), q_{max} and $X^2_m r$ for divalent metal ions ($n = 5$) (b) and q_{max} and $|\log K_{OH}|$ for transition metal ions ($n = 5$) (c).

Table 7
Regression models of relationship between q_{max} and metal ion characteristics for divalent metal ions ($n = 5$)

Model (q_{max} =)	R^2	R^2_{adj}	SE	F	p	MAPE
4. $0.053X^2_m r + 0.096$	0.928	0.904	0.021	78.365	0.003	7.214
5. $0.328\ X_m + 0.042$	0.731	0.649	0.038	17.566	0.025	13.057
6. $0.001AW + 0.088$	0.666	0.569	0.043	13.298	0.036	14.190
7. $0.035Z^* - 0.312$	0.671	0.576	0.047	13.591	0.035	13,797
8. 0.403r(Å)−0.105	0.557	0.438	0.056	8.831	0.059	14.395
9. $0.582 - 0.074Z^2/r$	0.701	0.613	0.038	15.437	0.029	15.619
10. $0.022AN/\Delta IP + 0.112$	0.548	0.428	0.050	8.555	0.061	15.792
11. $0.229\ X_m + 0.019\ Z^*$-0.508	0.983	0.967	0.012	117.596	0.008	3.202
12. $0.023Z^* - 0.037|\log K_{OH}| - 0.171$	0.910	0.824	0.026	20.662	0.046	8.300

and the former parameters ($X^2_m r$,AW, Z^*) showed greater fitness (Table 7) ($\alpha = 0.005$). Most parameters such as $X^2_m r$, AW, X_m, Z^*, r(Å), AN/ΔIP were positively correlated with metal uptake capacities, and Z^2/r was inversely correlated with q_{max}. Some similar results were reported by Tobin et al. [44], and they found that the amount of uptake of divalent cations was directly related with ionic radius r(Å). $X^2_m r$ was still the best fitting variable ($R^2_{adj} = 0.847$, MAPE = 8.542) (Fig. 2(b)). And from Table 7, we can realize that appropriate bivariate models generally could increase the imitative effect (model. 11 and 12).

3.3.3. Models for transition metal ions

This study selected divalent metal ions (Cd^{2+}, Cr^{3+}, Cu^{2+}, Zn^{2+}, Ni^{2+}) to build models as revealed in Table 8. Several dissimilar ionic characteristics such as $|\log K_{OH}|$, IP, Z/r^2, Z/AR^2 became statistical significant ($\alpha = 0.005$). Among them metal uptake capacities only increased with the decreasing of $|\log K_{OH}|$, and the most valuable parameter ($R^2_{adj} = 0.871$, MAPE = 2.169) shown in Fig. 2(c). It was also noted from model 19-22 that two-variable model had greater ability to improve the fitting results. A combination of Z/r^2 and $|\log K_{OH}|$ provided the best fit.

Z/r^2, Z/AR^2 Z/r and Z^2/r were different forms of the cation-polarizing power, which presented the strength of ion interaction of metal and cells. Padeste [45] reported carbonate with transition metal ions was easier to hydrolyze than ions II A and I A. Cation-polarizing power and $|\log K_{OH}|$ were inversely correlated. Ion hydrolysis ability enhanced with cation-polarizing power increasing and resulting to the reduction of $|\log K_{OH}|$. From Table 8, we can infer that ion hydrolysis played an important role in biosorption of metal especially transition metal. The close connection between q_{max} and ionization potential indicated that transition metals had unfilled valence shell and better electron affinity.

The best univariate model 13 showed $|\log K_{OH}|$ could explain 87% variation of q_{max}, and mean

Table 8
Regression models of relationship between q_{max} and metal ion characteristics for transition metal ions ($n = 5$)

Model (q_{max} =)	R^2	R^2_{adj}	SE	F	p	MAPE
13. 0.296-$|\log K_{OH}|$0.011	0.903	0.871	0.000	57.016	0.005	2.169
14. $0.005Z^2/r + 0.171$	0.597	0.485	0.145	10.182	0.049	12.121
15. $0.003IP + 0.119$	0.769	0.699	0.011	21.359	0.019	8.843
16. $0.038Z/r^2 + 0{,}049$	0.709	0.623	0.039	15.998	0.028	9.725
17. $0.209Z/AR^2 - 0.057$	0.700	0.612	0.400	15.363	0.030	10.074
18. $0.077Z/r$-0.023	0.790	0.726	0.033	23.956	0.016	6.913
19. $0.366 - 0.003Z^2/r$-0.016$|\log K_{OH}|$	0.955	0.910	0.008	23.625	0.041	1.985
20. $0.378 - 0.008Z/r^2$–0.016$|\log K_{OH}|$	0.999	0.999	0.001	1350.2	0.001	0.267
21. $0.396 - 0.041Z/AR^2 - 0.016|\log K_{OH}|$	0.998	0.997	0.001	1213.7	0.001	0.283
22. $0.008IP$-$0.065Z/AR^2 + 0.119$	0.903	0.810	0.008	19.037	0.049	2.450

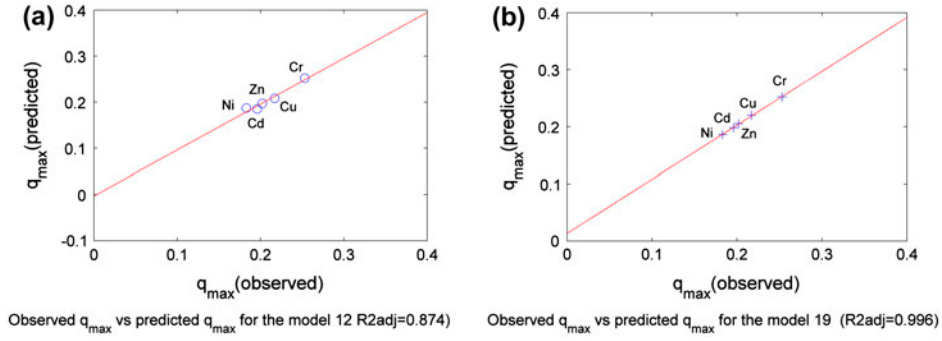

Fig. 3. Observed q_{max} vs. predicted q_{max} for the model 13 ($R^2_{adj} = 0.874$) (a) and Observed q_{max} vs. predicted q_{max} for the model 20($R^2_{adj} = 0.996$) (b).

absolute percent error was only 2.169. Therefore, the value of observed q_{max} and predicted q_{max} were very close (Fig. 3(a)). That two-variable model 20 had more predictive ability than 13 (Fig. 3(b)) It presented these QICAR models could predict metal uptake capacity according to metal ionic characteristics excellently.

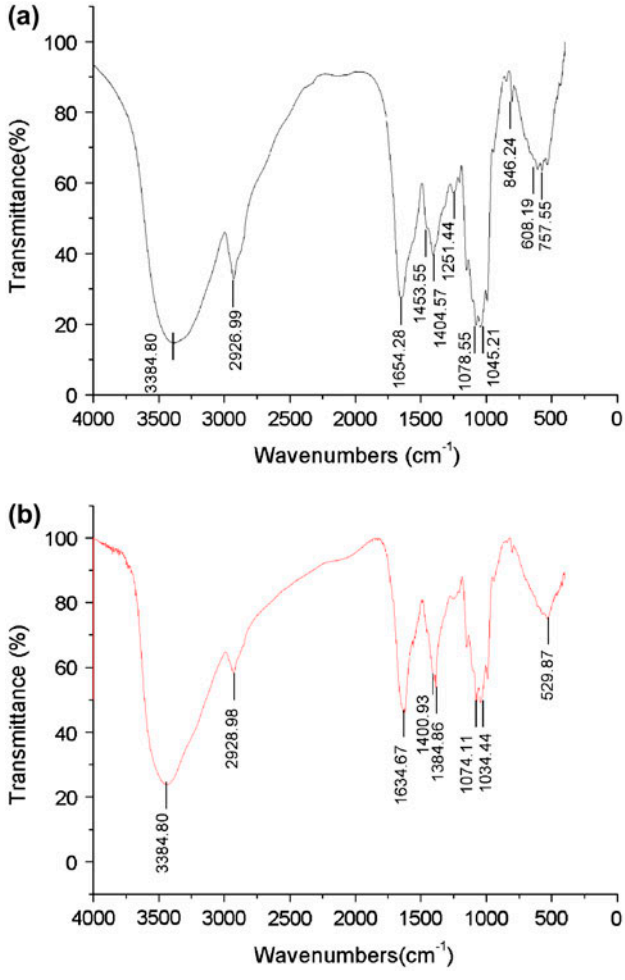

Fig. 4. FT-IR spectra of the intact *P. eryngii*(a) and *P. eryngii* with lead nitrate solution (200 mg l^{-1}) (b).

3.4. Fourier transform-infrared analysis

FT-IR spectra of the control biomass (metal free) were shown in Fig. 4(a). The absorption band at 3,384 cm^{-1} was assigned to the shake-up adsorption peak of –OH and $–NH_2$ groups on the adsorbent surfaces (v (–OH) and v ($–NH_2$)) [46]. The peak at 2,926 was due to aliphatic hydrocarbons symmetric stretching [47]. The formation of the band at 1,630 cm^{-1} was typical for γC=O of amide. And the peaks at 1,453–1,404 cm^{-1}, 1,251–1,204 cm^{-1} represented C–N stretching vibration of amino acid. In 4.b, the FT-IR patterns of Pb^{2+} loaded samples showed that the peak shift from 3,384 to 3,439 cm^{-1} suggesting possible interaction between amino group and Pb^{2+} [16]. After contacting with Pb^{2+}, both peak wave numbers of two adsorbents at 1,251 and 1,204 cm^{-1} decreased. The IR spectra before and after Pb^{2+} binding presented that amide I, II, IV, and sulfamide groups were involved in Pb^{2+} binding. The carboxyl band position shifted from 1,453 to 1,400 cm^{-1} and 1,404 to 1,384 cm^{-1} after biosorption of Pb^{2+} which also indicated that carboxyl group interacts with Pb^{2+}.

Conclusion

In the present study, *P. eryngii* performed well as metal cations absorbent.

Medium biomass loading, contact time, and pH were found to be key factors to affect removal Pb^{2+} and Cd^{2+}.

FT-IR spectra of biomass of *P. eryngii* before and after Pb^{2+} biosorption showed that amino/amido, sulfamide and carboxyl groups interacted with Pb^{2+} and major contribution was due to N-containing groups.

The metal uptake capacity of *P. eryngii* was $Pb^{2+} > Cr^{3+} > Cu^{2+} > Zn^{2+} > Cd^{2+} > Ni^{2+} > K^{+}$ calculated by the Langmuir isotherm model. QICAR models could successfully correlate biosorption capacity with metal ionic characteristics.

In the 22 ion properties r(Å), AN, ΔE_0(V), ΔIP(eV), X_m, $|\log K_{OH}|$, $X_m^2 r$, Z^2/r, AN/ΔIP, σp, OX, AR, AW, IP, AR/AW, Z^*,Z^{*2}/r, N, Z/r^2, Z/AR^2, Z/r, Z/AR, Covalent Index Value displayed excellent linear correlation with q_{max} for all tested metal ions. It could be inferred that convalent binding principally affect surface biosorption.

Appropriate classified metal ions could improve connection between ionic characteristics and biosorption capacity. Divalent metal ions and transition metal ions both presented significant linear relations with more ionic properties which might explain different biosorption principles of different metal ions. QICAR models could predict metal uptake capacity according to metal ionic characteristics excellently.

Acknowledgments

This study financially supported by the National 863 High Technology Research and Development Program of China (NO.2006AA06Z361), Science and Technology Supportive Project of Sichuan Province, China (NO.2013SZ0062), and Science and Technology Supportive Project of Chengdu (No.12DXYB087JH-005). The authors wish to thank Professor Guanglei Cheng and Dong Yu from Sichuan University for their technical assistance.

References

[1] S. Larous, A.H. Meniai, M.B. Lehocine, Experimental study of the removal of copper from aqueous solutions by adsorption using sawdust, Desalination 185 (2005) 483–490.
[2] C. Wang, J. Liu, Z. Zhang, B. Wang, H. Sun, Adsorption of Cd(II), Ni(II), and Zn(II) by tourmaline at acidic conditions: Kinetics, thermodynamics and mechanisms, Ind. Eng. Chem. Res. 51 (2012) 4397–4406.
[3] S. Rengaraj, S.H. Moon, Kinetics of adsorption of Co(II) removal from water and wastewater by ion exchange resins, Water Res. 36 (2002) 1783–1793.
[4] C. Chen, J. Wang, Influence of metal ionic characteristics on their biosorption capacity by *Saccharomyces cerevisiae*, Appl. Microbiol. Biotechnol. 74 (2007) 911–917.
[5] V. Prigione, M. Zerlottin, D. Refosco, V. Tigini, A. Anastasi, G.C. Varese, Chromium removal from a real tanning effluent by autochthonous and allochthonous fungi, Bioresour. Technol. 100 (2009) 2770–2776.
[6] M. Tsezos, Biosorption of metals. The experience accumulated and the outlook for technology development, Hydrometall. 59 (2001) 241–243.
[7] A. Mansri KIB, J. François, Chromium removal using modified poly(4-vinylpyridinium) bentonite salts, Desalination 245 (2009) 95–107.
[8] J.J. Hostýnek, P.S. Magee, Fragrance allergens classification and ranking by QSAR, Toxicology in Vitro 11 (1997) 377–384.
[9] D.J.W. Blum, R.E. Speece, Determining chemical toxicity to aquatic species, Environ. Technol. 24 (1990) 284–293.
[10] M.C. Newman, J.T. McCloskey, Predicting relative toxicity and interactions of divalent metal ions Microtox bioluminescence assay, Environ. Toxicol. Chem. 15 (1996) 275–281.
[11] J.D. Walker, M. Enache, J.C. Dearden, Quantitative cationic–activity relation- ships for predicting toxicity of metals, Environ. Toxicol. Chem. 22 (2003) 1916–1935.
[12] H.T Wolterbeek, T.G. Verburg, Predicting metal toxicity revisited general properties vs. specific effects, Sci. Total Environ. 279 (2001) 87–115.
[13] B. Thomas, U.Y. Kinraide, A scale of metal ion binding strengths correlating with ionic charge, Pauling electronegativity, toxicity, and other physiological effects, J. Inorg. Biochem. 101 (2007) 1201–1213.
[14] M.C. Newman, J.T. McCloskey, C.P. Tatara, Using metal-ligand binding characteristics to predict metal toxicity quantitative ion character–activity relationships (QICARs), Environ. Health Perspect. 106 (1998) 1419–1425.
[15] C.P. Tatara, M.C. Newman, J.T. McCloskey, P.L. Williams, Use of ion characteristics to predict relative toxicity of mono-, di- and trivalent metal ions *Caenorhabditis elegans* LC50, Aquat. Toxicol. 42 (1998) 255–269.
[16] S.S. Zamil, S. Ahmad, M.H. Choi, J.Y. Park, S.C. Yoon, Correlating metal ionic characteristics with biosorption capacity of *Staphylococcus saprophyticus* BMSZ711 using QICAR model, Bioresour. Technol 100 (2009) 1895–1902.
[17] J. Remacle, The cell wall and metal binding, In: B. Volesky (Ed.), Biosorption of Heavy Metals, CRC press, Boca Raton, 1990, pp. 7–44.
[18] B. Volesky, Removal and recovery of heavy metals by biororption, In: B. Volesky (Ed.), Biosorption of Heavy Metals, CRC press, Boca Rat on, pp. 7–44, 1990.
[19] S.V. Avery, J.M. Tobin, Mechanism of adsorpt ion of hard and soft metal ions to *Saccharomyces cerevisiae* and influence of hard and soft anions, Applied Environ. Microbiol. 59 (1993) 2851–2856.
[20] O.D. Uluozlu, A. Sari, M. Tuzen, M. Soylak, Biosorption of Pb(II) and Cr(III) from aqueous solution by lichen (*Parmelina tiliaceae*) biomass, Bioresour. Technol. 99 (2008) 2972–2980.
[21] S.Y. Wang, M.H. Tsai, S.F. Lo, M.J. Tsai, Effects of manufacturing conditions on the adsorption capacity of heavy metal ions by Makino bamboo charcoal, Bioresour. Technol. 99 (2008) 7027–7033.
[22] X. Jing, Y. Cao, X. Zhang, D. Wang, X. Wu, H. Xu,Biosorption of Cr(VI) from simulated wastewater using a cationic surfactant modified spent mushroom, Desalination 269 (2011) 120–127.
[23] Y. Cao, Z. Liu, G. Chen, X. Jing, H. Xu, Exploring single and multi-metal biosorption by immobilized spent Tricholoma lobayense using multi-step response surface methodology, Chem. Eng. J. 164 (2010) 183–195.
[24] A. Sari, M. Tuzen, Kinetic and equilibrium studies of biosorption of Pb(II) and Cd(II) from aqueous solution by macrofungus (*Amanita rubescens*) biomass, J. Hazard. Mater. 164 (2009) 1004–1011.
[25] I. Kiran, T. Akar, S. Tunali, Biosorption of Pb(II) and Cu(II) from aqueous solutions by pretreated biomass of *Neurospora crassa*, Process Biochem. 40 (2005) 3550–3558.
[26] M.E.R. Carmona, M.A.P. da Silva, S.G. Ferreira Leite, Biosorption of chromium using factorial experimental design, Process Biochem. 40 (2005) 779–788.
[27] T. Sahan, H. Ceylan, N. Sahiner, N. Aktas, Optimization of removal conditions of copper ions from aqueous solutions by *Trametes versicolor*, Bioresour. Technol. 101 (2010) 4520–4526.
[28] L.S. De Lima, M.D.M. Araujo, S.P. Quináia, D.W. Migliorine, J.R. Garcia, Adsorption modeling of Cr, Cd and Cu on activated carbon of different origins by using fractional factorial design, Chem. Eng. J. 166 (2011) 881–889.

[29] D.F.V. Lewis, M. Dobrota, M.G. Taylor, Metal toxicity in two rodent species and redox potential: Evaluation of quantitative structure-activity relationships, Environ. Toxicol. Chem. 18 (1999) 2199–2204.
[30] Y.T. Zhang, X. Sun, The structural data mining of solubility of metallic sulphide, Comput. Appl. Chem. 21 (2004) 690–694.
[31] N.L. Iskandar, N.A.I.M. Zainudin, S.G. Tan, Tolerance and biosorption of copper (Cu) and lead (Pb) by filamentous fungi isolated from a freshwater ecosystem, J. Environ. Sci. 23 (2011) 824–830.
[32] W. Huang, Z. Liu, Biosorption of Cd(II)/Pb(II) from aqueous solution by biosurfactant-producing bacteria: Isotherm kinetic characteristic and mechanism studies, Colloids Surf. B 105 (2013) 113–119.
[33] A. Kogej, A. Pavko, Comparison of *Rhizopus nigricans* in a pelleted growth form with some other types of waste microbial biomass as biosorbents for metal ions, World J. Microbiol. Biotechnol. 17 (2007) 677–685.
[34] A. Sari, D. Mendil, M. Tuzen, M. Soylak, Biosorption of Cd (II) and Cr(III) from aqueous solution by moss (*Hylocomium splendens*) biomass: Equilibrium, kinetic and thermodynamic studies, Chem. Eng. J. 144 (2008) 1–9.
[35] R.G. Pearson, Hard and soft acids and bases, Am. Chem. Soc. 85 (1963) 3533–3539.
[36] E. Nieboer, D.H.S. Richardson, The replacement of the nodescript term 'heavy metals' by a biological and chemically significant classification of metal ions, Environ. Pollut. B 1 (1980) 3–26.
[37] S.V. Avery, J.M. Tobin, Mechanism of adsorption of hard and soft metal ions to *Saccharomyces cerevisiae* and influence of hard and soft anions, Appl. Environ. Microbiol. 59 (1993) 2851–2856.
[38] O. Raize, Y. Argaman, S. Yannai, Mechanisms of biosorption of different heavy metals by brown marine macroalgae, Biotechnol. Bioeng. 87 (2004) 451–458.
[39] M.J. Brady, J.M. Tobin, Binding of hard and soft metal ions to *Rhizopus arrhizus* biomass, Enzyme Microb. Technol. 17 (1994) 791–796.
[40] C. Chen, J. Wang, Correlating metal ionic characteristics with biosorption capacity using QSAR model, Chemosphere 69 (2007) 1610–1616.
[41] E. Nieboer, W.A.E. McBryde, Free-energy relationships in coordination chemistry. III. A comprehensive index to complex stability, Can. J. Chem. 51 (1973) 2512–2524.
[42] J. Bayo, Kinetic studies for Cd(II) biosorption from treated urban effluents by native grapefruit biomass *Citrus paradisi* L.): The competitive effect of Pb(II), Cu(II) and Ni(II), Chem. Eng. J. 191 (2012) 278–287.
[43] A. Saeed, M.W. Akhtar, M. Iqbal, Affinity relationship of heavy metal biosorption by the husk of *Cicer arientinum* (Chickpea var. black gram) with their atomic weights and structural features, Fresenius Environ. Bull. 14 (2005) 219–223.
[44] J.M. Tobin, D.G. Cooper, R.J. Neufeld, Uptake of metal ions by *Rhizopus arrhizus* biomass, Appl. Environ. Microbiol. 47 (1984) 821–824.
[45] A.R.C. Padeste, H.R. Oswald, The influence of transition metals on the thermal decomposition of calcium carbonate in hydrogen, Mater. Res. Bull. 25 (1990) 1299–1350.
[46] L. Zhirong, A. Uddin, S. Zhanxue, FT-IR and XRD analysis of natural Na-bentonite and Cu(II)-loaded Na-bentonite, Spectrochim. Acta A Mol. Biomol. Spectrosc. 79 (2011) 1013–1016.
[47] W.J. Liu, F.X. Zeng, H. Jiang, X.S. Zhang, Adsorption of lead (Pb) from aqueous solution with Typha angustifolia biomass modified by $SOCl_2$ activated EDTA, Chem. Eng. J. 170 (2011) 21–28.